

# Fabrication of hollow titania microspheres with tailored shell thickness

Mukesh Agrawal · Andrij Pich ·  
Nikolaos E. Zafeiropoulos · Manfred Stamm

Received: 13 December 2007 / Accepted: 17 December 2007 / Published online: 8 January 2008  
© Springer-Verlag 2007

**Abstract** Submicron hollow spheres are an interesting class of materials that receive significant attention nowadays. Closed and mechanically robust homogeneous hollow titania microspheres with as much shell thickness as 130 nm were fabricated by coating polystyrene beads with titania nanoparticles using sol–gel chemistry and subsequently removing the core either via heating or a chemical dissolution process. The thickness of the titania shell deposited on polystyrene core was finely tuned between 100 and 130 nm by varying the concentration of titania precursor, i.e.,  $\text{Ti}(\text{OEt})_4$  salt from 0.5 to 2 mM during the coating process. The obtained hybrid core–shell particles and hollow microspheres were characterized by scanning electron microscopy, transmission electron microscopy, infrared spectroscopy, X-ray diffraction, and thermogravimetric analysis. The approach employed is well suited to the preparation of titania-coated polystyrene hybrid particles and hollow titania spheres, which can find their applications as novel building blocks with unique optical properties for fabrication of advanced materials, catalyst, and drug delivery system.

**Keywords** Titania nanoparticles · Polystyrene beads · Hybrid particles · Hollow spheres

## Introduction

Hollow spheres represent a special class of materials, which offers interesting prospects in a wide spectrum of potential applications such as protection of light-sensitive components and biologically active agents (proteins, enzymes, or DNAs), chromatography, catalysis, coatings, composites and fillers, waste removal, nanoreactors and large biomolecular release systems [1–3]. Among all the ceramics, a great deal of effort has been devoted to the fabrication of hollow titania spheres. This material is well known for its unique properties (such as high refractive index, good surface chemistry, resistance to discoloration under ultraviolet light, and photo catalytic activity, etc.) which makes it suitable for a number of applications such as in photonic band gaps [4], catalysts [5], white pigments [6, 7] nanoreactors [8], chemical sensors, energy conversion, sorption media, and filters [9].

A variety of chemical and physicochemical strategies, including heterophase polymerization combined with a sol–gel process [10, 11], nozzle-reactor systems [12, 13], emulsion or interfacial polymerization strategies [14–16], surface living polymerization process [17–19], and self-assembly techniques [20–22] has been employed to fabricate polymeric or ceramic hollow spheres. Some of them are of particular interest and hence have been used most frequently to fabricate these nanostructures with tailored properties. The first one is layer-by-layer (LBL) approach introduced by the pioneering work of Caruso and coworkers [1, 23–26]. Submicrometer-sized colloidal particles are coated with multilayered shells by the sequential

M. Agrawal (✉) · N. E. Zafeiropoulos · M. Stamm (✉)  
Leibniz-Institut für Polymerforschung Dresden e.V.,  
Hohe Strasse 6,  
01069 Dresden, Germany  
e-mail: agrawal@ipfdd.de  
e-mail: stamm@ipfdd.de

A. Pich  
Institut für Makromolekulare Chemie und Textilchemie,  
Technische Universität Dresden,  
Mommsenstr. 4,  
01062 Dresden, Germany

adsorption of polyelectrolytes and oppositely charged nanoparticles. Calcination of the obtained core–shell particles results in the fabrication of hollow spheres. The major advantage of this method is its lack of specificity for the combination of core and shell materials rendering it applicable to a wide range of systems. However, the method is not entirely free of problems like layers are added in time consuming discrete steps, which consist of the repeated adsorption of polyelectrolytes and nanoparticles, centrifugation, water washing, and re-dispersion cycles. Secondly, a large amount of redundant polymer is incorporated in the shell during the multiple absorption of alternating polyelectrolytes layers on colloidal latex particles. The second approach involves templating of the sol–gel precursors of nanoparticles against crystalline arrays of colloidal nano–micro spheres [27, 28]. In this process, the template is coated with a thin layer of the ceramic material by the infiltration of its precursor through the colloidal assemblies, thus resulting in core–shell particles. Subsequently, these core–shell particles are turned into hollow spheres by calcination at elevated temperatures in air or selective etching in an appropriate solvent. This approach has also been reported to suffer from a number of limitations; the most prominent one is tailoring the pore morphology of macro-porous materials. Fine control of pore wall thickness and the formation of structures with closed pores have been difficult to achieve because reaction of alkoxides to produce metal oxides results in the production of large amount of water and alcohol. Removal of the produced water and alcohol during drying and heat treatment results in large shrinkage and the formation of cracks in the materials [29]. Another approach, which is considered as the most common and simplest way to prepare hybrid–hollow particles, is the use of functionalized colloid particles as templates for nanoparticle deposition (including gold [30], CdS [31], mesoscale ZnS [32] or polymer beads [33–35]) in solution. This methodology involves coating of the template particles with inorganic shell by either controlled surface precipitation of inorganic molecule precursors (silica, titania, etc.) or direct surface reactions utilizing specific functional groups on the cores. The template particles are afterwards removed by either core dissolution or calcination to generate ceramic hollow spheres. Considerable efforts have been made for the preparation of titania-coated polymer spheres using this approach [5, 10, 36].

The above described pioneering works are very interesting but unfortunately, when it comes to the fabrication of titania hollow spheres, these approaches have been reported to be accompanied with some disadvantages, such as the formation of irregular coatings, aggregation of the coated particles, low efficiency of controlling the coating thickness, and formation of secondary titania particles [37]. This

can be attributed to the relatively high activity of titania precursors than those of other ceramic materials. Thus, despite of prior extensive work on titania hollow spheres, it is still a challenge to develop a facile, fast, and feasible method to prepare hollow titania spheres with uniform, dense, and thick ceramic walls. For certain applications mentioned above, hollow spheres with a porous and mechanically robust shell are required which can allow the controlled transport of target species across it. However, for extremely large target species such as enzymes and proteins, the sizes of the pores present within the shell have to be made comparable to the size of those molecules. Presence of such a large-sized pore in thin ceramic walls deteriorates their mechanical strength and limits their use in such applications [25, 26].

In this study, we demonstrated a simple, fast, but effective approach to fabricate hollow titania spheres via templating titania nanoparticles against polystyrene beads using sol–gel approach. The presented system not only overcomes the problems realized previously in the way to hollow titania spheres but also allows us to perform nanoengineering with these nanostructures in terms of their size, morphology, and shell thickness. The beauty of this system lies in following facts: (1) To our best knowledge, this is the first sol–gel method which enables us to synthesize smooth and uniform titania shell of as much thickness as 130 nm on polystyrene beads, without preparation of secondary titania nanoparticles. Deposition of such a thick titania layer on polystyrene core makes it possible to achieve porous and mechanically robust hollow titania spheres. A number of methods are reported in literature [10, 38, 39] which describes fabrication of titania shell with at the most 80-nm thickness. Beyond this limit, it is very difficult to control the thickness, uniformity, and roughness of titania shell using these approaches. (2) It offers a great deal of control over the thickness of the titania shell which can easily be tuned through the variation in concentration of titanium salt, i.e.,  $\text{Ti}(\text{OEt})_4$  in formulations. (3) In contrast to the multistep LBL approach [1, 23–26], it offers a fast and facile way to the polystyrene–titania hybrid particles and hollow titania spheres. (4) There is no need to synthesize nanoparticles separately prior to perform coating process.

## Experimental

**Materials** Styrene (ST; Fluka) and acetoacetoxyethylmethacrylate (AAEM; 97%; Aldrich) were passed through an inhibitor removal column and then vacuum distilled under nitrogen before use. Titanium ethoxide (85%; Acros), ammonium hydroxide (28–30%  $\text{NH}_3$  in water; Acros), and acetic acid (100%; Merck) were used without addi-

tional purification. Distilled water was employed as the polymerization medium.

**Synthesis of polystyrene particles** Monodisperse- and  $\beta$ -diketone-functionalized polystyrene particles with an average diameter of 540 nm were synthesized by surfactant-free emulsion polymerization as reported earlier by our group [40]. In a typical process, 170 g of water and appropriate amounts of styrene (19 g) and AAEM (1 g) were introduced into a double-wall glass reactor equipped with mechanical stirrer, reflux condenser, nitrogen inlet, and temperature controller. After deoxygenating the reaction mixture via bubbling of the nitrogen gas for 30 min, temperature was increased to 70 °C and aq. SPDS solution (0.3 g in 10-g water) was added into it to start the polymerization process. The reaction was allowed to proceed for another 24 h and polystyrene latex particles were obtained as a stable dispersion in water with approximately 10% solid content.

**Synthesis of polystyrene–titania hybrid particles** The coating reaction was carried out in ethanol at 70 °C by hydrolyzing the titanium ethoxide in the presence of the  $\beta$ -diketone-functionalized polystyrene particles. In a typical process, variable amounts of titanium ethoxide (See Table 1) were mixed into 10 g of extra-pure ethanol and the mixture was refluxed at 70 °C for 2 h. Subsequently, 1 g of latex containing 10 wt.% polystyrene particles was added into the reaction media followed by the addition of four to five drops of glacial acetic acid as precipitating agent. After reacting for 20 h, hybrid particles were cleaned by three cycles of centrifugation–re-dispersion in ethanol and water respectively.

**Synthesis of hollow titania spheres by dissolution of polystyrene core** The polystyrene cores were removed by adding an amount of titania-coated polystyrene spheres in ethanol to an excess of tetrahydrofuran (THF). After 10 h, the obtained particles were centrifuged two times at 10,000 rpm for 10 min by re-dispersing in THF in order to ensure the complete removal of the polystyrene core. Finally, hollow spheres were transferred to ethanol via two more centrifugation–re-dispersion cycles.

**Table 1** Variation in size of titania-coated hybrid particles and their titania shell thickness with change in the concentration of  $\text{Ti}(\text{OEt})_4$  salt in formulation

S. No.	Sample Name	Concentration of $\text{Ti}(\text{OEt})_4$ salt (mM)	Size of hybrid particles (nm)	Titania shell thickness (nm)
1	Sample 1	0.5	740	100
2	Sample 2	1	760	110
3	Sample 3	1.5	780	120
4	Sample 4	2	800	130

**Synthesis of hollow titania spheres by calcinations** In addition to the dissolution process described above, it was also possible to remove the polystyrene cores by calcination of the titania-coated polystyrene particles in a furnace at elevated temperature [10]. In the first step, few drops of ethanolic suspension of hybrid particles were placed on cleaned glass slide and dried initially at room temperature and subsequently at 60 °C for 1 h. Finally, the glass plate was placed inside a furnace and heated to 550 °C in air at 5°C/min heating rate. After 3 h, the sample was allowed to cool down to room temperature.

**Characterization methods** Particle size measurements were carried out on Zetasizer 2000, Malvern Instruments. The average value of at least three measurements was taken as the particle diameter at room temperature. Scanning electron microscopy (SEM) images were taken on a Gemini microscope (Zeiss, Germany) at an accelerating voltage of 4 kV. Prior to analysis, samples were coated with thin Au/Pd layer to increase the contrast and quality of the images. Transmission electron microscopy (TEM) images were recorded on a Zeiss Omega 912 microscope at 160 kV. Thermo-gravimetric analysis (TGA) was performed on a Q 500 analyzer from TA Instruments. Before measurements, samples were dried in vacuum for approximately 48 h and then were heated in platinum crucibles in 25–700 °C temperature range with nitrogen as carrier gas at 5 K/min heating rate. X-ray diffractometer (XRD) spectra were taken by analyzing the powdery samples on a HZG 4/A-2 (Seifert FPM) X-ray diffractometer. Infrared spectra were recorded with Mattson Instruments Research Series 1 Fourier transform infrared (FTIR) spectrometer. Prior to analysis, dried samples were mixed with KBr and pressed to form a tablet.

## Results and discussion

**Polystyrene core particles** Polystyrene particles functionalized with  $\beta$ -diketone groups have been prepared via surfactant-free co-polymerization of ST and AAEM. Due to its hydrophilic character, AAEM is located predominantly on the surface of emulsion droplets during the co-polymerization process and hence stabilizes the obtained colloidal system as well as provides the  $\beta$ -diketone functionality to polystyrene beads. In addition, this method offers an effective control over the size of polystyrene beads by varying the amount of AAEM co-monomer in the reaction media [40]. Figure 1a shows SEM image of polystyrene beads indicating that particles are monodisperse in size with quite smooth surface. The average diameter of the polystyrene particles was measured as 540 nm. *Dynamic light scattering (DLS) measurements of these template particles are shown in “Appendix 1.”* The

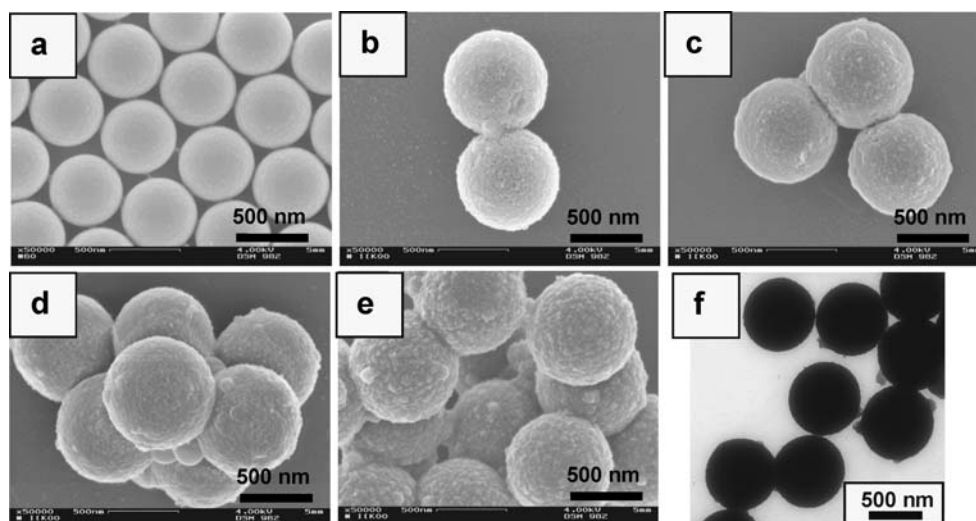
same polystyrene beads have been successfully employed in our previous investigations for the deposition of zinc oxide [41], maghemite [42], and zinc sulfide [43] nanoparticles.

**Titania-coated polystyrene spheres** SEM images of titania-coated polystyrene spheres produced at different concentrations of  $\text{Ti}(\text{OEt})_4$  salt are shown in Fig. 1b–e. These images illustrate the presence of a thick but smooth, homogenous and complete titania shell on polystyrene beads. Moreover, one can observe that coated particles are monodisperse in size and spherical in shape similar to the neat polystyrene beads, employed as template. *DLS measurements of these particles are shown in “Appendix 1.”* When coating reaction was performed at 0.5-mM titanium ethoxide concentration, the size of polystyrene beads increased from 540 nm (neat polystyrene) to 740 nm as determined by TEM, yielding the titania shell of 100-nm thickness (thickness of the deposited titania shell is half of the increment in total diameter of the particles after coating process). When concentration of titania salt was gradually increased further from 0.5 to 2 mM (as shown in Table 1), it resulted in the increase in size of coated particles from 740 to 800 nm (giving shell thickness in the range of 100–130 nm). Figure 1f illustrates TEM image of sample 2 which reveals that titania-coated particles are monodisperse in size and possess a complete titania shell on polystyrene core. TGA analysis of the coated particles revealed a continuous increase in their titania contents in the range of 16–48 wt.%, with increase in the concentration of titanium ethoxide salt employed during the synthesis (shown in “Appendix 2”). These data are in good agreement with SEM analysis, illustrating that observed increment in thickness of hybrid particles is due to the deposition of increased amount of titania nanoparticles on template surface.

In contrast to the results reported in literature [10, 38, 39, 44], we achieved a gradual increase in the size of coated

particle with increasing the concentration of titania salt in formulations till the titania shell reaches a thickness of 130 nm. Moreover, no secondary titania particle formation and no deviation from the spherical shape of hybrid particles were observed even at the highest dose of titanium ethoxide. This can be attributed to chemistry used in the preparation of template particles as well as precipitation of titania shell on these polymeric beads. As mentioned earlier, template particles were prepared by the co-polymerization of styrene with AAEM. This added co-monomer renders a fair amount of active sites ( $\beta$ -diketone groups) to the template surface, which provides its hydrophilicity and captures most of the titania nanoparticles, available in reaction media for coating process. Moreover, the synthesis of titania nanoparticles was carried out by a controlled hydrolysis of  $\text{Ti}(\text{OEt})_4$  salt, catalyzed by acetic acid. We believe that presence of acetic acid in reaction media played a crucial role in deposition of a thick, smooth, and uniform titania layer on template surface. Acetic acid not only catalyses the reaction but also serves as chelating titania particles on template surface [45]. Same observations were made agent to stabilize the hydrolysis–condensation process and minimize the aggregation of by Wu and Yeh [46] in preparation of titanium dioxide nanoparticles. In order to support this fact, we carried out some reaction sets using hydrochloric acid, water, or  $\text{NH}_4\text{OH}$  as catalyst. It resulted into the nonuniform coating of polystyrene beads, high surface roughness, and presence of secondary titania particles (see “Appendix 3”). A closer look of Fig. 1 reveals that there is no significant change in the surface roughness of PS- $\text{TiO}_2$  composite particles while increasing the  $\text{Ti}(\text{OEt})_4$  concentration from 0.5 to 1.5 mM. However, particles prepared at highest  $\text{Ti}(\text{OEt})_4$  concentration (2 mM) are relatively rough than those prepared at lower concentrations. It can be attributed to the relatively fast hydrolysis of titania precursor at highest concentration of  $\text{Ti}(\text{OEt})_4$  salt. It is well known that hydrolysis of metal oxides salts is proportional to

**Fig. 1** SEM images of **a** polystyrene beads and polystyrene–titania hybrid particles prepared at different  $\text{Ti}(\text{OEt})_4$  concentrations: **b** sample 1; **c** sample 2; **d** sample 3; **e** sample 4 and **f** TEM image of sample 2





the concentration of reactants [47]. We speculate that rate of precipitation of titania shell at 2-mM concentration of Ti (OEt)<sub>4</sub> salt is too fast to form a smooth shell of polystyrene core. We have observed the same phenomena while in the precipitation of ZnO shell of polystyrene core in our previous study [41]. The reaction parameters which accelerate to the rate of hydrolysis of the precursor cause the deposition of rough shell on polystyrene beads.

**Hollow titania sphere** It has been reported in the literature that polystyrene core could be removed from the hybrid particles by suspending them in toluene followed by two centrifugation–re-dispersion cycles [48, 49]. After dispersing in toluene, all the polystyrene are expected to come out into solution leaving behind porous and hollow spheres. Produced hollow spheres were transferred into ethanol for characterization. Figure 2 shows TEM micrographs of sample 3 before and after the chemical dissolution of polystyrene core.

In agreement with SEM data, in the case of hybrid particles, a uniform coating of titania layer on polystyrene beads was observed. A noticeable difference in contrast of TEM images of titania-coated polystyrene particles taken before and after the chemical treatment (because of the difference in electron density) confirms that hollow titania spheres were produced. The successful formation of hollow titania spheres confirms the high uniformity of titania coating on polystyrene templates.

Figure 3 illustrates SEM images of hollow titania spheres produced via chemical dissolution (Fig. 3a,b) and calcination (Fig. 3c,d) of titania-coated hybrid particles. Figure 3a,b illustrates that chemical treatment of sample 2 and sample 4 resulted in complete and intact hollow spheres. We note that, in the case of sample 4 (Fig. 3b), the obtained particles were deliberately crushed (by applying force to them) [39, 49] prior to the SEM analysis to prove that particles are hollow in nature. One can clearly see the cavities (shown by dashed arrows) and broken pieces (shown by solid arrows) of titania shell of these hollow structures.

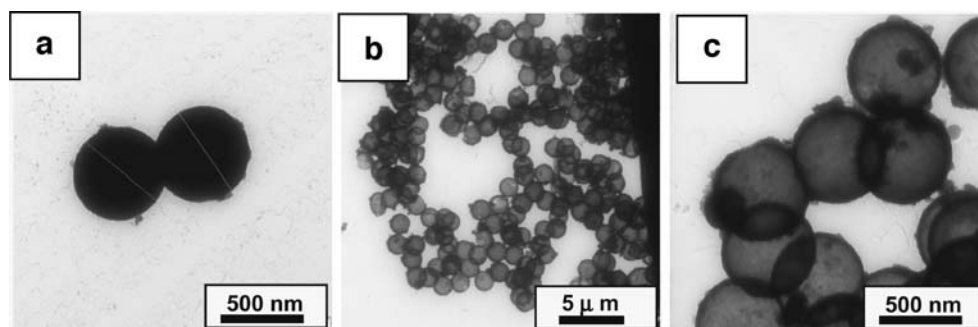
Moreover, it can also be observed that produced hollow particles are spherical in shape and monodisperse in size. *DLS measurements of these hollow titania spheres are depicted in “Appendix 1”*. Imhof [10] observed deformation of hollow

titania spheres after removal of polystyrene core via chemical dissolution method because of the thin layer of titania shell (50 nm). Similarly, Wang et al. [48] observed spreading as well as creases and folds in hollow titania spheres of comparable diameter, produced by the same method as Imhof [10]. On the contrary, in our case, the high thickness of titania shell (100–130 nm) accounted for a good mechanical strength of the ceramic wall of hollow spheres, thus maintaining the shape of the template particles.

Calcination of titania-coated polystyrene particles in air at elevated temperature also resulted in the fabrication of hollow titania spheres [39, 50]. Figure 3c,d shows SEM images of hollow titania spheres obtained after calcination of sample 2 and sample 4 in a furnace at elevated temperature. The samples were prepared by drying a drop of the suspension of titania-coated hybrid particles on a glass slide before calcination. These images reveal that calcination results in formation of intact, monodisperse, and spherical hollow structures with thick shell walls. In the case of sample 2, again particles were deliberately crushed before analysis to confirm their hollow nature. The cavity of hollow titania spheres (broken arrow) and broken pieces of titania shell (solid arrow) can be observed in Fig. 3c. Calcination of polystyrene particles coated with relatively thin titania layer has been reported to produce relatively a large fraction of damaged hollow spheres [10, 23, 49]. On the contrary, in this study most of the produced hollow spheres were found intact and unbroken because of the sufficient shell thickness.

The diameter of hollow titania spheres produced by calcination, was found to be 10–20% smaller than those of uncalcined hybrid particles. In some studies more than 30% or even around 44% shrinkage has been observed after calcination, probably because of thin ceramic shell [44, 48, 49]. On the contrary, the hollow spheres produced in the present study have thick titania shells with high two-dimensional anisotropy, which renders them stable during the heat treatment. Consequently, only a slight shrinkage was observed for our hollow spheres, and this may be attributed to sintering contraction of the nanoparticles. Hollow spheres without significant shrinkage can be favorable for some applications where accurately controlled sizes are of pivotal importance.

**Fig. 2** **a** TEM image of titania-coated polystyrene particles; sample 3 and **b** low and **c** high magnified TEM images of hollow titania spheres obtained after chemical dissolution of polystyrene core from sample 3



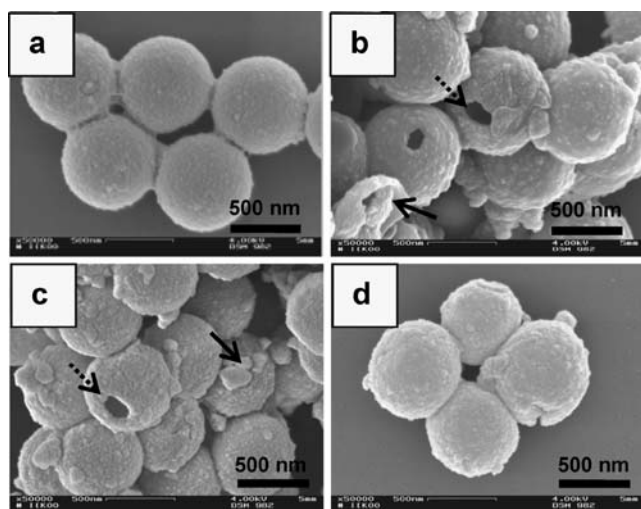


**Fig. 3** SEM images of hollow titania spheres obtained after chemical dissolution of polystyrene core from **a** sample 2 and **b** sample 4 and calcination of **c** sample 2 and **d** sample 4. In **b** and **c**, solid arrows show the broken pieces of titania shell produced by the deliberate crushing of hollow spheres and dashed arrows show the cavities of hollow particles

To verify removal of polystyrene core from hybrid particles, produced hollow spheres were analyzed by FTIR spectroscopy and resulting spectra were compared with that of titania-coated particles (see Fig. 4). In the case of hybrid particles, one can observe presence of C–H stretching bend at around  $3,000\text{ cm}^{-1}$ , aromatic C–C stretch at around  $1,470\text{ cm}^{-1}$ , C–H out-of plane bend at  $765\text{ cm}^{-1}$ , and aromatic C–C out-of-plane bend at  $700\text{ cm}^{-1}$ . Aromatic overtones are visible in the range of  $1,700\text{--}2,000\text{ cm}^{-1}$ . All these peaks are characteristic peaks of polystyrene, which have almost disappeared in the case of toluene-treated hollow particles, indicating that most of the polystyrene has been removed by this process [10, 38].

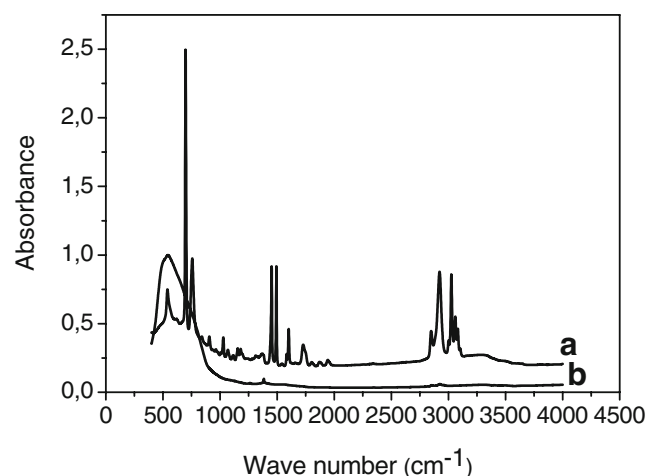


**Fig. 4** FTIR spectra of (a) titania-coated polystyrene particles (sample 2) and (b) hollow titania spheres, produced after chemical dissolution of polystyrene core from sample 2

Figure 5a displays the X-ray diffraction pattern of titania-coated polystyrene powder (sample 4) dried at room temperature under vacuum. It demonstrates that, during the coating process, almost amorphous phase of titania is deposited on polystyrene core. The diffraction peaks which appeared in this XRD pattern (Fig. 5a) could be associated to the reflections (210) and (111) of brookite phase or to the reflection (110) of rutile phase of titania. Same observations have been reported in literature while preparation of  $\text{TiO}_2$  nanoparticles in similar reaction conditions employed in this study [51, 52]. Figure 5b illustrates XRD pattern of the same sample after calcination at  $5^\circ\text{C}/\text{min}$  to  $550^\circ\text{C}$  for 3 h. All the diffraction peaks of this calcined sample in Fig. 5b can be indexed to a pure hexagonal anatase phase of  $\text{TiO}_2$ , with calculated cell constants of  $a=b=3.785\text{ \AA}$  and  $c=9.514\text{ \AA}$ . The peak intensities and peak positions are in good agreement with expected literature values [53]. The indices and spacings for the diffraction rings are (1) 101,  $0.353\text{ nm}$ ; (2) 004,  $0.236\text{ nm}$ ; (3) 200,  $0.189\text{ nm}$ ; (4) (105+211),  $0.167\text{ nm}$ ; (5) 204,  $0.151\text{ nm}$ ; and (6) 116,  $0.134\text{ nm}$ , respectively. Moreover, it can be observed that XRD pattern of hollow titania spheres (Fig. 5b) has also a noticeable background, which reveals the presence of significant amount of amorphous titania phase still in this sample. It can be explained on the basis of the fact that presence of the organic residue in the hybrid particles obstructed the coagulation of titania nanoparticles, resulting in a more restricted-imperfect crystallization [50].

We propose the physical interaction between  $\beta$ -diketone groups, located on the surface of colloidal templates and titania precursors (formed in reaction media) as driving force for precipitation of titania layer on polystyrene beads. As per the literature [47], preparation of  $\text{TiO}_2$  nanoparticles from titanium alkoxides, i.e.,  $\text{Ti}(\text{OR})_4$ , is thought to be composed of two stages. The first stage is a hydrolysis reaction, in

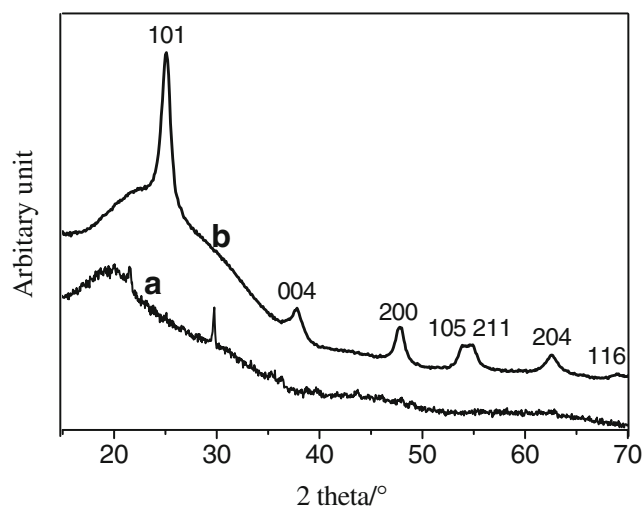


**Fig. 5** XRD pattern of (a) titania-coated polystyrene particles (sample 4) and (b) hollow titania spheres obtained after calcination of sample 4 at  $550^\circ\text{C}$

which alkoxide groups are replaced with hydroxide groups via an intermediate of expanded coordination number and titania precursors  $\text{Ti}(\text{OH})_x(\text{OR})_y$  are formed. Where  $x$  and  $y$  are the number of hydroxyl and alkoxy groups present on titanium atom in hydrolyzed product of titanium alkoxide and ( $x+y=4$ ). The second stage is a condensation–polymerization reaction where Ti–O–Ti bonds are formed from  $\text{Ti}(\text{OH})_x(\text{OR})_y$ , resulting in creation of three-dimensional structure, which precipitates out of the reaction solution. It has been reported in the literature [54, 55] that hydrolysis of titanium alkoxides in the presence of functionalized templates leads to the precipitation of titania nanoparticles preferentially on template surface because of the interaction between hydrolyzed monomer  $\text{Ti}(\text{OH})_x(\text{OR})_y$  and functionality of the template particles. As mentioned above, colloidal cores used in this study in the preparation of titania-coated hybrid particles are functionalized with  $\beta$ -diketone groups. Hence, as soon as the titania precursors are formed from  $\text{Ti}(\text{OEt})_4$  in reaction media, they are thought to be captured by templates via their interaction with  $\beta$ -diketone groups. Subsequently, condensation–polymerization process of adsorbed  $\text{Ti}(\text{OH})_x(\text{OR})_y$  species takes place resulting in precipitation of a titania layer on polystyrene core. Similar observations have been made by Fu and Qutubuddin [56] and Hanprasopwattana et al. [57]

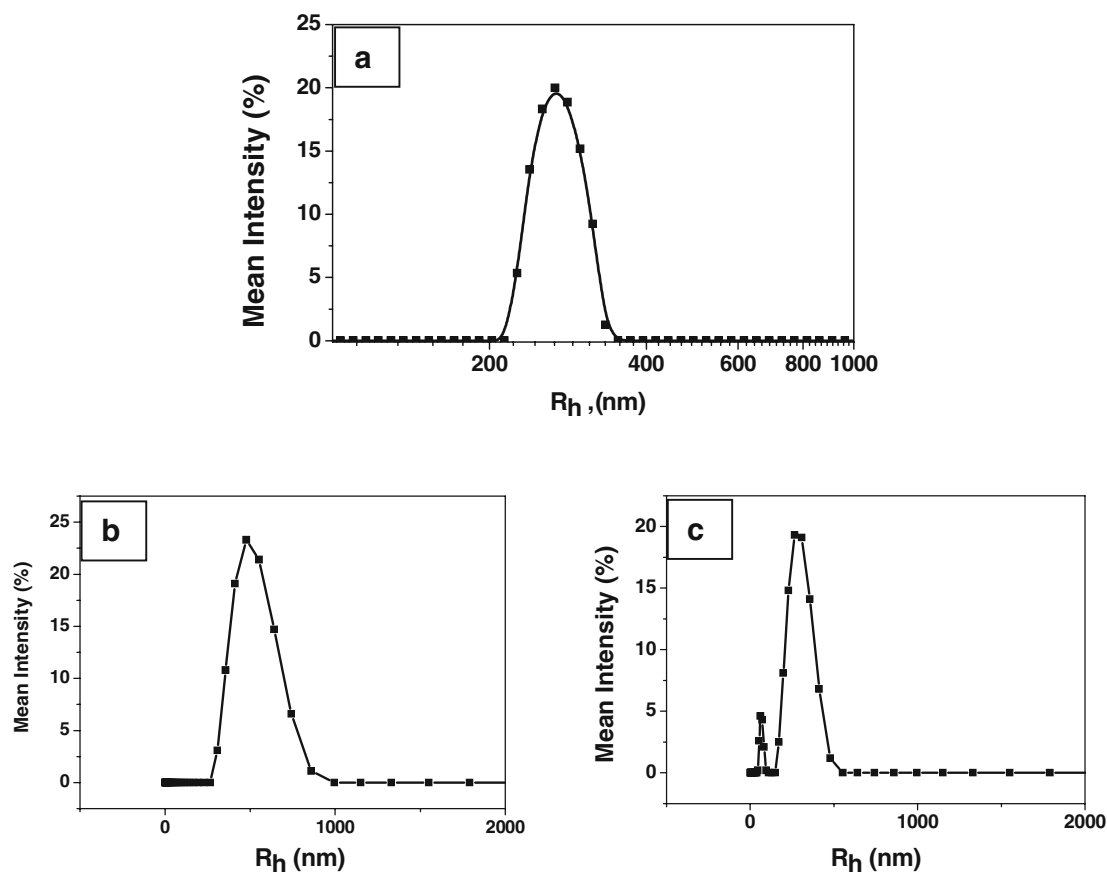
in the deposition of titania nanoparticles on silica spheres and Ocana et al. [58] on ZnO.

## Conclusions

In summary, we have demonstrated a simple but effective route to the monodisperse and intact hollow titania spheres with as much shell thickness as 130 nm. These hollow spheres have a well-defined void size that is determined by the diameter of the polystyrene template and a homogeneous shell whose thickness is mainly controlled by the concentration of the sol–gel precursor in reaction media. Although we only demonstrated this procedure with 540-nm polystyrene beads as examples, we believe that this method should be extendible to other colloidal templates of variable dimensions, and to hollow spheres made of other materials such as ZnO,  $\text{V}_2\text{O}_3$ ,  $\text{SnO}_2$ ,  $\text{Al}_2\text{O}_3$ , and  $\text{SiO}_2$ , etc.

**Acknowledgement** The authors are thankful to Mrs. Ellen Kern, Dr. Rudiger Häßler, Mr. Axel Mensch, and Dr. Dieter Jehnichen for helping out in SEM, TGA, TEM, and XRD measurements, respectively.

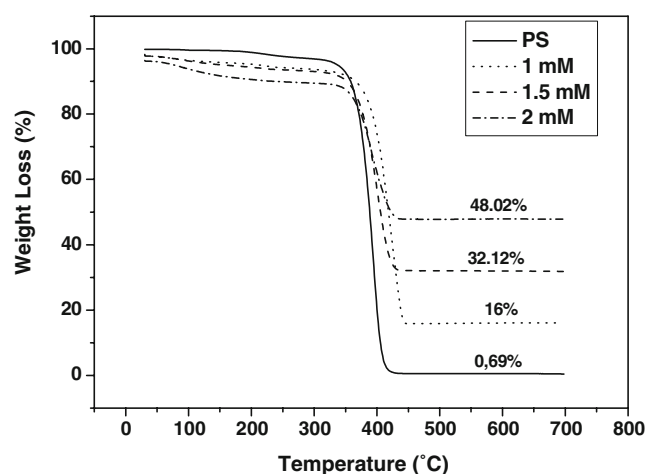
## Appendix 1



Dynamic light scattering measurements of (a) PS beads, (b) PS-TiO<sub>2</sub> composite particles (sample 4) and (c) hollow TiO<sub>2</sub> spheres obtained after the calcination of sample 4.

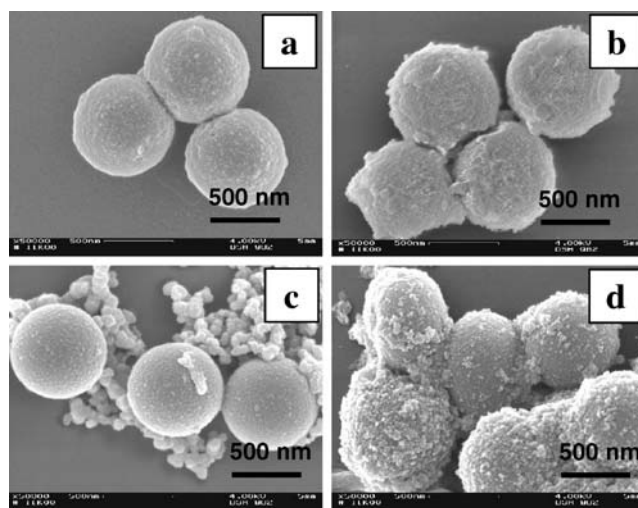
From these results, one can observe that there is no change in particle size distribution of PS beads after the coating of TiO<sub>2</sub> nanoparticles. The hydrodynamic radii has been found to increase from 270 to 475 nm after the precipitation of TiO<sub>2</sub> shell. However, these values are somewhat higher than those obtained from microscopic (SEM–TEM) analysis. In the case of hollow TiO<sub>2</sub> spheres, bimodal particle size distribution has been observed with the main peak at 365 nm. The appearance of small peak at 60 nm can be attributed to the broken pieces of hollow spheres. The damage of hollow spheres probably took place during dispersing these particle into water with the help of ultrasonic waves.

## Appendix 2



Thermo gravimetric traces of uncoated polystyrene particles and titania-coated polystyrene particles prepared at different Ti(OEt)<sub>4</sub> concentrations. In all cases, one can observe two main regions of weight loss: weight loss below 230 °C is due to the desorption of physically bonded water and removal of organic residue from sample and another one between 320 °C and 450 °C can be attributed to decomposition of polystyrene core. In the case of uncoated polystyrene particles, there was almost no residue at higher temperature region while coated polystyrene particles showed final residue ranging between 16% and 48%, which indicates their titania contents. As expected, final residue of titania-coated particles gradually increases as the employed concentration of the Ti(OEt)<sub>4</sub> salt increases.

## Appendix 3



SEM images of polystyrene–titania hybrid particles prepared by using different catalysts (a) CH<sub>3</sub>COOH, (b) NH<sub>4</sub>OH, (c) H<sub>2</sub>O and (d) HCl. These results reveal that CH<sub>3</sub>COOH is the suitable catalyst for the smooth and uniform coating of titania layer on polystyrene beads. In other cases, nonuniform coating, high surface roughness, and presence of secondary titania nanoparticles can be observed because of the fast hydrolysis of Ti(OEt)<sub>4</sub> salt.

## References

- Caruso F, Caruso RA, Mohwald H (1998) *Science* 282:1111–1114
- Jiang P, Bertone JF, Colvin VL (2001) *Science* 291:453–457
- Wilcox DL, Berg M, Bernat T, Kellerman D, Cochran JK (eds) (1995) *Hollow and solid spheres and microspheres: science and technology associated with their fabrication and application*. In: *Materials Research Society Proceedings*, Pittsburgh, vol. 372
- Nakamura H, Ishii M, Tsukigase A, Harada M, Nakano H (2005) *Langmuir* 21:8918–8922
- Zhang M, Gao G, Zhao DC, Li ZY, Liu FQ (2005) *J Phys Chem B* 109:9411–9415
- Hsu WP, Yu R, Matijevic E (1993) *J Colloid Interface Sci* 156:56–65
- Haq I, Matijevic E (1993) *Colloid Surf A* 8:153
- Li J, Zeng HC (2005) *Angew Chem Int Ed* 44:4342
- Hagfeldt A, Grätzel M (1995) *Chem Rev* 95:49–68
- Imhof A (2001) *Langmuir* 17:3579
- Tissot I, Reymond JP, Lefebvre F, Bourgeat-lami E (2002) *Chem Mater* 14:1325
- Lu Y, Fan H, Stump A, Ward TL, Rieker T, Brinker CJ (1999) *Nature* 398:223
- Iida M, Sasaki T, Watanabe M (1998) *Chem Mater* 10:3780
- Bruinsma PJ, Kim AY, Liu J, Baskaran S (1997) *Chem Mater* 9:2507
- Fowler CE, Khushalani D, Mann S (2001) *Chem Commun* 19:2028
- Rana RK, Mastai Y, Gedanken A (2002) *Adv Mater* 14:1414



17. Zhou Q, Wang S, Fan X, Advincula RC (2002) *Langmuir* 18:3324
18. Perruchot C, Khan MA, Kamitsi A, Armes SP, von Werne T, Patten TE (2001) *Langmuir* 17:4479
19. von Werne T, Patten TE (2001) *J Am Chem Soc* 123:7497
20. Discher BM, Won YY, Ege DS, Lee JCM, Battes FS, Discher DE, Hammer DA (1999) *Science* 284:1143
21. Zhao M, Sun L, Crooks RM (1998) *J Am Chem Soc* 120:4877
22. Wendland MS, Zimmerman SC (1999) *J Am Chem Soc* 121:1389
23. Caruso RA, Sussha A, Caruso F (2001) *Chem Mater* 13:400–409
24. Caruso F, Spasova M, Sussha A, Giersig M, Caruso RA (2001) *Chem Mater* 13:109–116
25. Wang D, Caruso RA, Caruso F (2001) *Chem Mater* 13:364–371
26. Ji L, Ma J, Zhao C, Wei W, Ji L, Wang X, Yang M, Lu Y, Yang Z (2006) *Chem Commun* 11:1206
27. Zhong Z, Yin Y, Gates B, Xia Y (2000) *Adv Mater* 12:206–209
28. Kawahashi N, Matijevic E (1991) *J Colloid Interface Sci* 143:103
29. Subramanian G, Manoharan VN, Throne JD, Pine DJ (1999) *Adv Mater* 11:1261
30. Liz-Marzan LM, Giersig M, Mulvaney P (1996) *Chem Commun* 6:731
31. Wu D, Ge X, Zhang Z, Wang M, Zhang S (2004) *Langmuir* 20:5192
32. Velikov K, Blaaderen AV (2001) *Langmuir* 17:4779
33. Graf C, Vossen DLJ, Imhof A, van Blaaderen A (2003) *Langmuir* 19:6693
34. Tissot I, Novat C, Lefebvre F, Bourgeat-lami E (2001) *Macromolecules* 34:5737
35. Yang M, Ma J, Zhang C, Yang Z, Lu Y (2005) *Angew Chem Int Ed* 44:2
36. Yang ZZ, Niu ZW, Lu YF (2003) *Angew Chem Int Ed* 42:1943
37. Guo X-C, Dong P (1999) *Langmuir* 15:5535
38. Cheng X, Chen M, Wu L, Gu G (2006) *Langmuir* 22:3858–3863
39. Wang P, Chen D, Tang F-Q (2006) *Langmuir* 22:4832–4835
40. Pich A, Bhattacharya S, Adler H-JP (2005) *Polymer* 46:1077
41. Agrawal M, Pich A, Zafeiropoulos NE, Gupta S, Pionteck J, Simon F, Stamm M (2007) *Chem Mater* 19:1845–1852
42. Choi H-J, Jang LB, Lee JY, Pich A, Bhattacharya S, Adler H-JP (2005) *IEEE Trans Magn* 41:3448
43. Pich A, Hain J, Prots Yu, Adler H-JP (2005) *Polymer* 46:7931
44. Wang L, Sasaki T, Ebina Y, Kurashima K, Watanabe M (2002) *Chem Mater* 14:4827–4832
45. Aelion R, Loebel A, Eirich F (1950) *J Am Chem Soc* 72:5705–5712
46. Wu JCS, Yeh CY (2001) *J Mater Res* 16:615
47. Park J, Myoung J, Kyong, J, Kim H (2003) *Bull Korean Chem Soc* 24:671
48. Wang D, Caruso F (2002) *Chem Mater* 14:1909–1913
49. Caruso F, Caruso RA, Mohwald H (1999) *Chem Mater* 11:3309–3314
50. Zhang M, Gao G, Li C-Q, Liu F-Q (2004) *Langmuir* 20:1420–1424
51. Bokhim, Morales A, Novaro O (1995) *J Mater Res* 10:2788
52. Kumar KNP, Keizer K, Burggraaf AJ (1994) *J Mater Sci Lett* 13:59–61
53. Bryan JD, Heald SM, Chambers SA, Gamelin DR (2004) *J Am Chem Soc* 126:11640
54. Zhang D, Yang D, Zhang H, Lu C, Qi L (2006) *Chem Mater* 18:3477–3485
55. Cheng H, Ma J, Zhao Z, Qi L (1995) *Chem Mater* 7:663
56. Fu X, Qutubuddin S (2001) *Colloid Surf A Physicochem Eng Aspects* 178:151–156
57. Hanprasopwattana A, Srinivasan S, Sault AG, Datye AK (1996) *Langmuir* 12:3173–3179
58. Ocana M, Hsu WP, Matijevic E (1991) *Langmuir* 7:2911